J. Fluid Mech. (1997), *vol.* 334, *pp.* 293–314

Measurement of turbulence near shear-free density interfaces

By E. L. G. KIT[1], E. J. STRANG[2] AND H. J. S. FERNANDO[2]

[1]Department of Fluid Mechanics and Heat Transfer, Tel-Aviv University, Ramat-Aviv 69978, Israel

[2]Environmental Fluid Dynamics Program, Department of Mechanical and Aerospace Engineering, Arizona State University, Tempe, AZ 85287-6106, USA

(Received 1 May 1995 and in revised form 3 September 1996)

The results of an experimental study carried out to investigate the structure of turbulence near a shear-free density interface are presented. The experimental configuration consisted of a two-layer fluid medium in which the lower layer was maintained in a turbulent state by an oscillating grid. The measurements included the root-mean-square (r.m.s.) turbulent velocities, wavenumber spectra, dissipation of turbulent kinetic energy and integral lengthscales. It was found that the introduction of a density interface to a turbulent flow can strongly distort the structure of turbulence near the interface wherein the horizontal velocity components are amplified and the vertical component is damped. The modification of r.m.s velocities is essentially limited to distances smaller than about an integral lengthscale. Inspection of spectra shows that these distortions are felt only at small wavenumbers of the order of the integral scale and a range of low-wavenumbers of the inertial subrange; the distortions become pronounced as the interface is approached. Comparison of the horizontal velocity data with the rapid distortion theory (RDT) analyses of Hunt & Graham (1978) and Hunt (1984) showed a qualitative agreement near the interface and a quantitative agreement away from the interface. On the other hand, the RDT predictions for the vertical component were in general agreement with the data. The near-interface horizontal velocity data, however, showed quantitative agreement with a model proposed by Hunt (1984) based on nonlinear vortex dynamics near the interface. The effects due to interfacial waves appear to be important for distances less than about 10% of the integral lengthscale. As a consequence of the non-zero energy flux divergence, the introduction of a density interface to oscillating grid turbulence increases the rate of dissipation in the turbulent layer except near the interface, where a sharp drop occurs. The present measurements provide useful information on the structure of turbulence in shear-free boundary layers, such as atmospheric and oceanic convective boundary layers, thus improving modelling capabilities for such flows.

1. Introduction

Density interfaces are widespread in nature, and often they coexist with contiguous turbulent layers. Interaction between density interfaces and turbulence is an important aspect of geophysical flow modelling because it leads to interfacial mixing and, consequently, determines the vertical buoyancy flux q through stratified layers. The vertical eddy diffusivity associated with the buoyancy flux, $k = -q/N^2$, where N is the buoyancy gradient or the buoyancy frequency (averaged over suitable vertical distances),

is an important input to the atmospheric and oceanic global circulation models and, hence, parameterization of q remains at the heart of geophysical microstructure research. Development of such parameterizations requires an understanding of mixing mechanisms as well as the nature of turbulence and wave fields at density interfaces. To this end, several laboratory experiments and theoretical/numerical studies have been reported on the simple case of turbulence–stratification interactions at mean shear-free density interfaces, and substantial progress has been made on various aspects of interfacial mixing. Of course, natural flow situations are more complex and contain both the effects of velocity shear and buoyancy forces. The shear-free case, however, can be considered as a precursor to understanding such complex situations.

Hunt (1984) proposed a technique for the analysis of the nature of steady shear-free turbulence near density interfaces (see also the related work of Hunt & Graham 1978). The approach involves the introduction of a density interface to a homogeneous turbulent velocity field (say defined by the root-mean-square (r.m.s.) velocity u_H and the lengthscale L_H) and calculation of the steady distorted flow field. Atmospheric measurements in zero-mean-flow convective boundary layers (e.g. Caughey & Palmer 1979) indicate that the averaged rate of turbulent kinetic energy dissipation, $\epsilon = \nu\overline{\omega^2}$, where ν is the kinematic viscosity and $\overline{\omega^2}$ is the mean-square of vorticity fluctuations, is approximately constant (within $\pm 20\%$) irrespective of the distance ξ below the inversion layer. Since the dissipation ϵ in the original homogeneous field (denoted as ϵ_H) satisfies $\mathrm{d}\epsilon_H/\mathrm{d}\xi = 0$ and since the velocity field resulting from the distortion of homogeneous turbulence by the interface also satisfies $\mathrm{d}\epsilon/\mathrm{d}\xi = 0$, with $\epsilon \to \epsilon_H$ when $\xi \to \infty$, it can be argued that the rate of dissipation ϵ_H should not be affected by the introduction of the density interface to homogeneous turbulence. Thus, to the first order, the introduction of the density interface does not alter vorticity fluctuations in the flow (also, the estimates of Hunt (1984) show that this is true for each individual wavenumber of the vorticity spectrum) and, therefore, the distortions can be considered as irrotational. The distortion to the velocity field can thus be represented as $\boldsymbol{u}^D = \nabla\phi$, where ϕ is the velocity potential. By writing the new velocity field near the interface as $\boldsymbol{u} = \boldsymbol{u}^H + \boldsymbol{u}^D$, where $\boldsymbol{u}^H$ is the velocity field in the absence of the interface, the techniques of rapid distortion theory (RDT) can be employed to calculate the distortion to the turbulence field; this was the approach employed by Carruthers & Hunt (1986, 1997), and Fernando & Hunt (1997) in calculating velocity fluctuations adjacent to shear-free density interfaces. It should be borne in mind that, to fully describe the processes near the interface, vorticity generation due to mechanisms such as baroclinic production, viscous effects and the distortion of small eddies by the large ones near the interface should be taken into consideration. Full nonlinear theories or sophisticated modelling studies are required to estimate the velocity fluctuations introduced by such mechanisms (e.g. Hunt 1984).

In the present work, extensive velocity measurements were made in a turbulent layer adjacent to a strong density interface, with the hope of understanding the influence of density interfaces on mixed-layer turbulence and providing experimental verifications for the underlying assumptions and predictions of certain analytical theories on turbulence near density interfaces. A mixing-box configuration employed in many previous studies was used (e.g. Turner 1968). Particular attention was paid to the following aspects:

(i) the assumption of Hunt (1984) that the introduction of a density interface to homogeneous turbulence does not lead to a change of the turbulent kinetic energy dissipation (except within a thin layer very near the wall where viscous and baroclinic effects may play an important role);

(ii) the modification of r.m.s. velocities and corresponding longitudinal wavenumber (k_1) spectra by the interface (similar measurements have been previously reported by McDougall 1979 and Hannoun, Fernando & List 1988 using laser-Doppler velocimetry (LDV), but only the frequency spectra have been measured);

(iii) the measurement of integral lengthscales and their variations with the distance from the interface; and,

(iv) the usefulness of the predictions of the RDT of Hunt & Graham (1978) and Hunt (1984) in describing the nature of oscillating grid turbulence near a density interface (the above theories are valid for homogeneous turbulence in the inviscid limit without any baroclinic vorticity production, and in practice these conditions are rarely met).

The velocity measurements were made using a rotating hot-film probe placed in the turbulent layer, with the turbulence driven by an oscillating grid. Measurements were carried out in the presence and absence of the interface so that the effects of the interface could be assessed and the properties of grid-induced turbulence could be further investigated. To obtain reliable estimates of the turbulent kinetic energy dissipation rate and spectra, the time series should be sufficiently long, but because of the slow time variations in the properties of the flow (e.g. entrainment at the interface) they should be short enough to avoid unsteady trends. As a compromise, relatively high density jumps (large Richardson numbers) were used to reduce the entrainment and to keep the interface relatively smooth without appreciable wave breaking events.

In §2 of this paper the experimental method is described, and experimental results are presented in §3. Section 4 is devoted to presenting turbulence measurements with and without interfaces and comparing them with existing theoretical ideas. A summary of the results is given in §5.

2. Experimental facility

The experiments were conducted in a tank of square cross-section with sides 47 cm and height 45 cm. The tank walls were constructed from 0.5 cm tempered glass to reduce the optical distortions that are usually encountered when using Plexiglas tanks with optical diagnostic techniques. A grid, made of 1.93 cm wide Plexiglas bars and a mesh (M) of 8 cm (solidity 42%), was supported in the tank by a stainless steel connecting rod (see figure 1*a*). The rod passed through a watertight seal located at the bottom of the tank and was driven by a DC motor via a slider crank mechanism. Three grid frequencies (f) of 2.15, 2.9 and 4.3 Hz and a single stroke of $S = 3.2$ cm were used. This range is rather narrow, but was found to be the best for trouble-free operation of the hot-film anemometer. The mean grid position z_B was set at 9 cm above the tank bottom; this distance was necessary to minimize the secondary currents induced within the tank. In a preliminary series of experiments, the distance z_B was systematically varied and the resulting flow patterns were studied by observing the motion of dye injected near the bottom and using LDV measurements (see Kit, Fernando & Brown 1995). The secondary mean flow observed for $z_B \geqslant 9$ cm was found to be less than 25% of the r.m.s. velocity.

The wavenumber spectra of the horizontal and vertical velocity components and the rate of turbulent kinetic energy dissipation ϵ were measured using two types of probes namely TSI conical and X-type hot-film probes. To provide the necessary mean flow, the hot film was mounted on a rotating arm that was designed to minimize probe vibrations by employing precision bearings and smooth belt drives. This arrangement

(*a*)

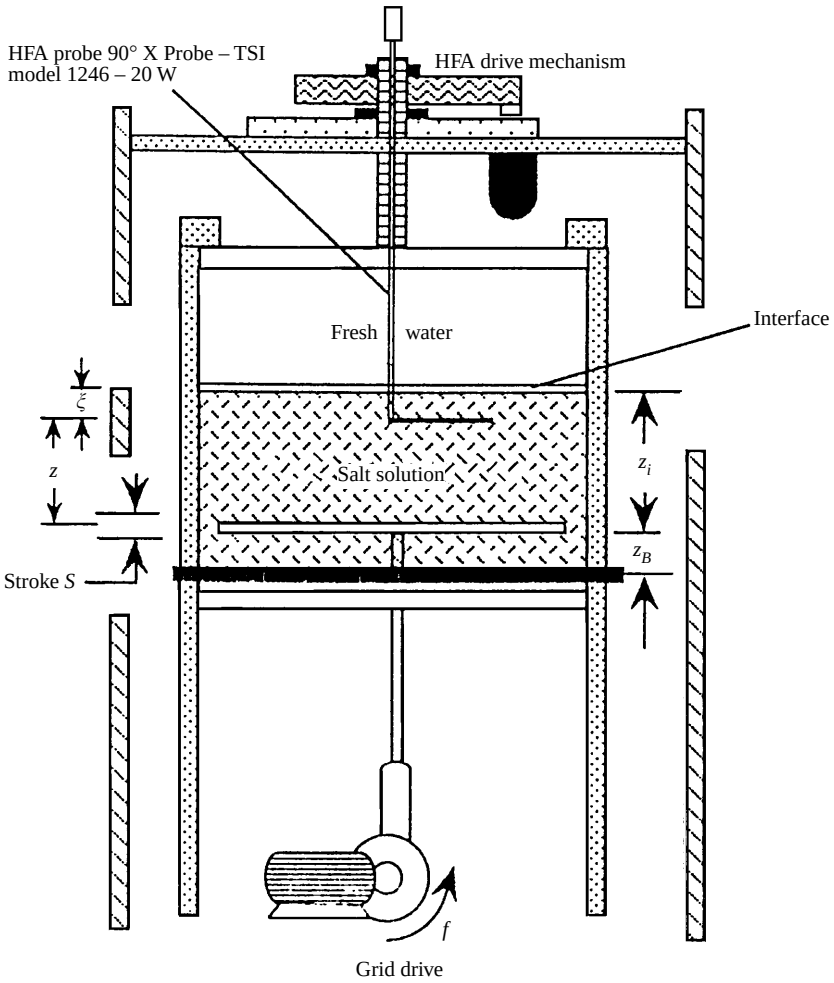

(*b*)

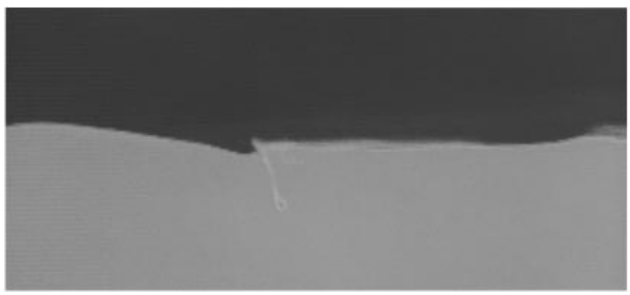

FIGURE 1. (*a*) A schematic of the experimental facility. (*b*) A photograph of the interface, taken using the LIF technique, at $Ri \sim 95$. Actual horizontal dimension of the field of view is 8 cm.

consisted of a stepping motor which is connected to an adjustable-tension belt drive that rotates a spindle carrying the hot film. Following a short spin-up period, the rotating arm achieves a constant angular speed and then comes to a stop after one revolution. Thereafter, it returns back to the original position and stays there for some time before the next set of data is taken; this procedure precludes probe measurements in its own wake and spin-up of fluid due to probe rotation (e.g. see Thompson & Turner 1975). The measurements made without grid oscillations clearly indicated that the time period between the probe runs (typically 30 s) is sufficient to ensure that the measurements are free from the wake effects of the previous run. The radius of the circle traced by the probe (17.2 cm) is much larger than the integral scales of turbulence ($\sim$ 2–3 cm), and hence no corrections were made for the curvature of the probe path (as in Thompson & Turner 1975). The x-direction referred to in the text is locally tangential to the arc transcribed by the probe tip.

In the experiments with two-layer stratification, the tank was filled with a salt solution in the lower layer and with fresh water (containing a minute amount of Rhodamine 6G) in the top layer. The grid was located in the bottom layer (see figure 1*a*). The typical density difference between the layers was maintained at $\Delta\rho = 0.1\rho_0$, where ρ_0 is the density of fresh water at room temperature. This provided a strong two-layer stratification (i.e. large Richardson number $Ri = \Delta b L_H/u_H^2$, where $\Delta b = \Delta\rho g/\rho_0$ is the buoyancy jump across the interface), thus yielding small entrainment rates and wave amplitudes at the interface.

The values of Ri used were in the range 90–150. The interfacial location was monitored by using two methods. In most of the experiments, a micro-scale conductivity probe was rapidly traversed vertically through the interface several times, before and after the velocity measurements, from which the averaged interfacial position was calculated. The accuracy of this method was checked using a few experiments in which an optical technique was used. Here the refractive indices of the upper and lower layers were matched using the technique described by Hannoun *et al.* (1988), and a uniform sheet of laser light (7 cm high, 0.6 mm thick) produced by a scanning mirror was shone through the interfacial area. The average position of the interface was calculated by tracking the constant concentration lines of Rhodamine 6G using the standard laser-induced fluorescence technique (LIF). The concentration contour representing the average concentration of the two layers was used for this purpose. Figure 1(*b*) shows a typical LIF photograph of the interface for the case of $Ri = 95$. The upper and lower layer fluids are denoted by different colours, and the mixed fluid is the bright line layer between them. Note the relative calmness of the interface, yet the presence of mixing events.

The distance between the mean position of the grid and the probe $z = h_{pr}$ was kept constant at $h_{pr} = 16$ cm $= 2M$, thus keeping an approximately constant value of turbulent intensity at the probe. Before the onset of grid oscillations, the hot-film probe was located 2–3 cm above the interface in the fresh-water layer. Due to the turbulent entrainment, the interface moved upward and, after some time, the probe was exposed to the turbulent layer. The velocity fluctuation measurements were made for different separations between the migrating interface and the fixed probe. The movement of the interface was very slow ($\leqslant 1$ mm min^{-1}) and, hence, the measurements can be considered as corresponding to a stationary state. This procedure allowed measurements of turbulence at any separation from the interface without changing the probe setting. Furthermore, entrainment at the interface ensures that it is sharp at the time of the measurements.

The velocity measurements were made by first setting the probe into motion at a

predetermined speed. A record of 1024 velocity points was acquired during the forward rotation of the probe. To enable proper ensemble averaging, the measurements were repeated several times, typically 20 to 40 realizations. To ensure the applicability of Taylor's hypothesis, the speed of the probe tip was adjusted so that it was about 10–20 times the r.m.s. velocity predetermined from a few test runs. A number of tests were conducted using different tip velocities to verify that the measured r.m.s. velocities and spectral measurements were independent of the probe velocity.

The longitudinal integral lengthscales of horizontal and vertical components of velocity in homogeneous water, $L_H^u (= L_H)$ and L_H^w, and the Taylor microscale λ were directly calculated from the data. The integral lengthscales were calculated by computing the auto-correlation function based on fluctuating horizontal (u) and vertical (w) velocity components, for example

$$R^{uu}(r) = \frac{\overline{u(x)u(x+r)}}{\overline{u^2}}, \tag{2.1}$$

and by obtaining the integral of $R^{uu}(r)$ to the first zero crossing. Here $\overline{u^2}$ is the variance of the velocity fluctuations and in homogeneous turbulence $u_H = (\overline{u^2})^{1/2}$. The Taylor microscale λ was calculated using (Tennekes & Lumley 1972, p. 67)

$$\epsilon = 15\nu \frac{\overline{u^2}}{\lambda^2}, \tag{2.2}$$

and the following procedure was used to evaluate the rate of dissipation ϵ.

At high frequencies, the u-component contained unwanted spikes making it unsuitable for the calculation of small-scale gradients (§3.4); thus, only the w-component was used for the calculation of ϵ. The calculations of the skewness factor (Tavoularis, Bennett & Corrsin 1978)

$$S_K = -\frac{\overline{(\partial u/\partial x)^3}}{\left[\overline{(\partial u/\partial x)^2}\right]^{3/2}} \tag{2.3}$$

for the u-component showed an average value of 0.31. This is somewhat lower than the commonly accepted value of 0.4, perhaps due to the noise contamination. The average S_K for the w-component was close to zero.

In calculating ϵ, local isotropy at small scales was assumed, and the expression

$$\epsilon = \tfrac{15}{2}\nu\overline{(\partial w/\partial x)^2} \tag{2.4}$$

was employed (Hinze 1975, pp.189, 219). The assumption of local isotropy in strongly stratified turbulent flows is questionable, but because the measurements were made below the interface in the homogeneous layer with comparatively high Reynolds numbers of turbulence ($R_\lambda = u_H\lambda/\nu \sim 70$), this assumption is reasonable. If $\epsilon = Au_H^3/L_H$, where A is a constant, then the ratio of the frequency scales of small-scale eddies $\left[\overline{(\partial u/\partial x)^2}\right]^{1/2}$ to anisotropic large eddies (u_H/L_H) near the interface becomes

$$\overline{(\partial u/\partial x)^2}^{1/2} \Big/ u_H/L_H = \left(A/15\right)^{1/2} Re^{1/2} = (A/15)R_\lambda \tag{2.5}$$

where $Re = u_H L_H/\nu$. When the above ratio is much greater than unity (or $R_\lambda \gg 1$), the small-scale eddies can be assumed to be independent of the large-scale anisotropy near the interface. Gargett, Osborn & Nasmyth (1984) proposed that small-scale dissipative eddies in stratified fluids are isotropic when $I = (\epsilon/\nu N^2)^{3/4} > 200$, where

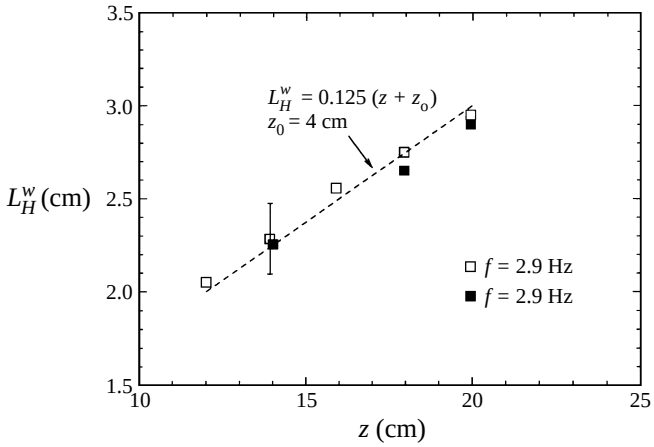

FIGURE 2. The longitudinal (x-direction) integral lengthscale for the vertical velocity component as a function of the distance from the grid. The dashed line corresponds to the linear relation $L_H^w = 0.125(z + z_0)$, where $z_0 = 4$ cm.

N is the local buoyancy frequency. Even just below the interface the buoyancy gradients are weak ($N \simeq 0.1\ \mathrm{s}^{-1}$), and typical values of I are on the order of 10^3, thus providing further justification for the use of the local-isotropy assumption.

The systematic calibration errors for the hot-film measurements were $\pm 0.5\%$ and the total cumulative errors of measurements were $\pm 15\%$ for ϵ and $\pm 10\%$ for the velocity and lengthscale.

3. Experimental results

3.1. *Integral lengthscale*

As stated before, a series of experimental runs was made in homogeneous water, as a precursor to the stratified runs, so that they could provide quantitative estimates of stratification effects. The longitudinal integral lengthscales of both velocity components L_H^u and L_H^w were evaluated using the hot-film velocity data. Note that, for isotropic turbulence, $L_H^u = 2L_H^w$, and L_H^u is usually considered as the typical integral lengthscale L_H in theoretical studies. The present measurements indicated that this relation is also approximately valid for oscillating-grid turbulence. The scatter of the data for L_H^u was rather high, however, possibly because of the probe vibration problems associated with the u-component. Therefore, only L_H^w was used for comparisons with stratified cases. The characteristic lengthscale L_H was evaluated via the measurement of L_H^w and using the above isotropic relation.

Figure 2 shows the variation of L_H^w as a function of the distance from the mean position of the grid, z. Note the increase of L_H^w with z, approximately following $L_H^w = \beta(z + z_0)$, with $\beta \simeq 0.125$ and the virtual origin $z_0 = 4$ cm. The dashed line indicates the least-squares fit to all of the data taken with different grid frequencies. According to Hopfinger & Toly (1976), the virtual origin usually lies below the grid mid-plane; this is in agreement with the above results. In general, the distance to the virtual origin from the mid-plane depends on various geometric parameters related to the grid. In addition, previous measurements show that the proportionality constant β depends strongly on the geometry of the grid and the stroke. For example, L_H^u measurements of Thompson & Turner (1975) show $L_H^u = 0.1(z + z_0)$ for $S = 1$ cm and

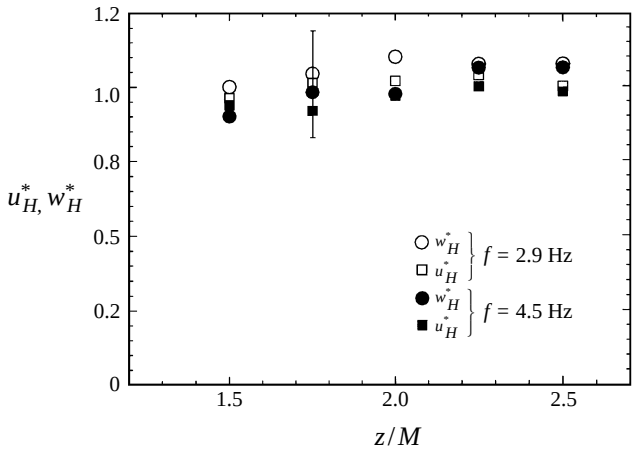

FIGURE 3. The distribution of the normalized vertical and horizontal r.m.s. velocity components as a function of the normalized distance for oscillating grid turbulence in homogeneous fluids.

$M = 5$ cm (i.e. $\beta = 0.05$) for grids with bars of both square and circular cross-section whereas the corresponding proportionality constant reported by Hopfinger & Toly (1976) was 0.125 for the $S = 4$ cm and $M = 5$ cm case (also see Hopfinger & Linden 1982). The present measurements of $\beta = 0.125$ for $S = 3.2$ cm indicate that β may not be a simple linear function of S as was assumed in Hopfinger & Linden (1982), but depends on a variety of factors related to the experimental configuration. The above empirical relation together with the Thompson & Turner (1975) result of $\beta = 0.05$ were found to underestimate the measurements of Brumley & Jirka (1987), who measured the grid turbulence both near and away from a free surface in an experimental tank similar to that used in the present study.

3.2. *R.m.s. velocities*

Figure 3 shows the normalized horizontal $u^*_H (= u_H/u_0)$ and vertical $w^*_H (= w_H/u_0)$ r.m.s. velocity fluctuations as a function of the distance z/M from the grid mid-plane, where the normalization variable u_0 is evaluated according to the empirical formula proposed by Hopfinger & Toly (1976) for the r.m.s. horizontal velocity in oscillating-grid turbulence, namely $u_0(z) = CS^{3/2}M^{1/2}f(z + z_0)^{-1}$, where z_0 is the virtual origin estimated from the lengthscale measurements. The results indicate that $C = 0.5$ is a good approximation for the present experiments, which is higher than the empirical value 0.25 proposed by Hopfinger & Toly (1976) based on their own data and those of Thompson & Turner (1975); however, their work indicates that C varies with the geometric parameters of the grid, if $S/M \leqslant 0.4$ and $S/d \leqslant 4$, which is the case for the present experiments. The values of C found by Hopfinger & Toly (1976) and Thompson & Turner (1975) are consistent and equal to 0.3 at small z where the above power law is valid. Also note that, for the bulk of the measurements, the w-component is usually larger than the u-component, which is expected as a consequence of uni-directional forcing of the grid. The anisotropy, w^*_H/u^*_H, however, does not exceed 1.1.

3.3. *Dissipation of turbulent kinetic energy*

The rate of dissipation of turbulent kinetic energy was measured using the method described in §2. Because of the possible noise contamination of the u-component in

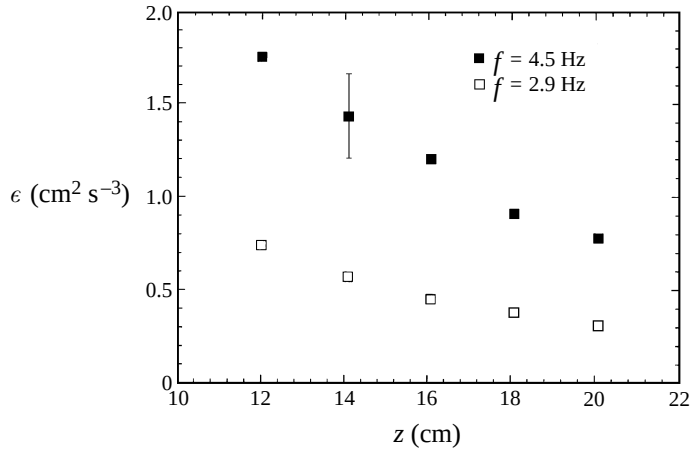

FIGURE 4. Dimensional rate of dissipation as a function of the distance from the oscillating grid, measured in homogeneous fluids.

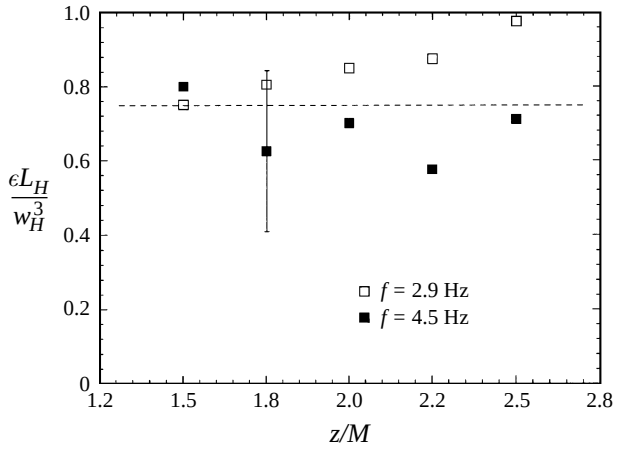

FIGURE 5. Normalized rate of dissipation as a function of the distance from the oscillating grid in homogeneous fluids.

the high-frequency spectral domain (see §3.4), it was not used for the calculations. Figure 4 shows a dimensional plot of measured ϵ versus distance z for two grid oscillation frequencies. The non-dimensional form of this plot, $\epsilon L_H/w_H^3$ versus z/M, is shown in figure 5. Note that the normalized dissipation rate $\epsilon L_H/w_H^3$ can be considered as constant in an approximate sense, and the average value of $\epsilon L_H/w_H^3$ is approximately 0.75 (as indicated by the dashed line). This is consistent with the commonly quoted values of $A \sim 1$ for high-Reynolds-number turbulence (Sreenavasan 1984). The observed variations sometimes fall outside the calculated error margin and possibly can be attributed to the weak secondary flows inherent in tank experiments. Note that if $L_H \propto z$ and $w_H \propto z^{-1}$, $\epsilon \sim w_H^3/L_H$ implies that $\epsilon \propto z^{-4}$.

Brumley & Jirka (1987) estimated the rate of dissipation in the oscillating-grid experiments by comparing their measured one-dimensional spectra with the Kol-

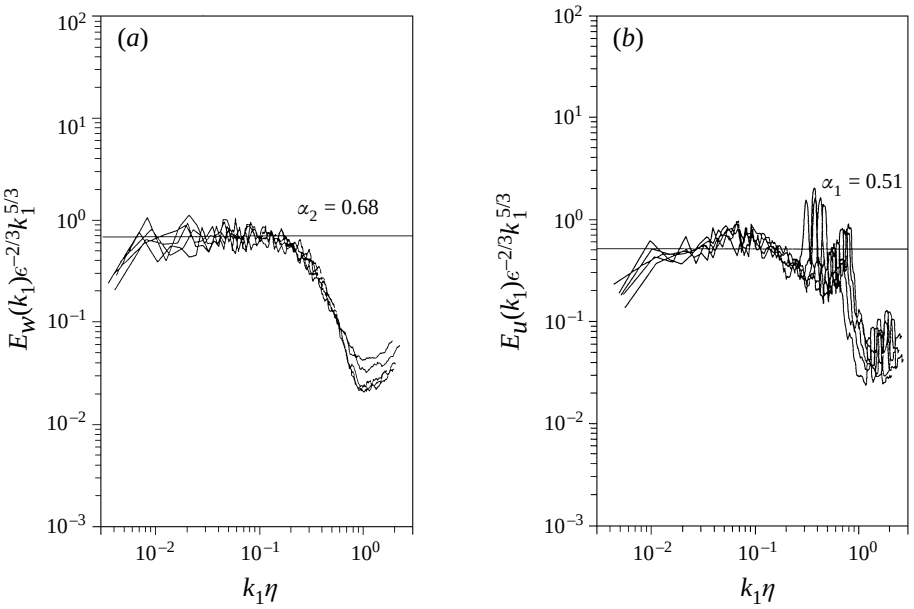

FIGURE 6. The normalized kinetic energy wavenumber (k_1) spectra measured by the hot-film anemometer in homogeneous fluids at $f = 2.9$ Hz. The five distances between the location of the hot-film probe and the oscillating grid vary in the range $z = 12-20$ cm $= 1.5M-2.5M$. (*a*) vertical velocity component, (*b*) horizontal velocity component.

mogorov inertial subrange form

$$E(k_1) = \alpha\epsilon^{2/3}k_1^{-5/3}, \tag{3.1}$$

where α is a constant and k_1 is the wavenumber in the x-direction. In the bulk of the turbulent layer, the measured spectra for u, $E_u(k_1)$, and w, $E_w(k_1)$, components gave approximately the same value of ϵ. Their comparison of this ϵ with that predicted by $\epsilon = Au_0^3/L_H^u$, where u_0 is calculated using the Hopfinger & Toly (1976) formula (with $C \simeq 0.25$) and L_H^u is calculated using the Thompson & Turner (1975) results, yielded $A \simeq 0.2$. Actual velocity and lengthscale measurements of Brumley & Jirka (1987) deviate from those of Hopfinger & Toly and Thompson & Turner, which may be attributed to this low value of A.

3.4. *Spectra*

The measured wavenumber spectra were compared with the one-dimensional Kolmogorov spectral form (3.1) for the inertial subrange. The established value of the constant α for $E_u(k_1)$, based upon previous works, is $\alpha = \alpha_1 = 0.51$ whereas it becomes $\alpha = \alpha_2 = 4\alpha_1/3 = 0.68$ for the lateral ($E_w(k_1)$) component (e.g. Comte-Bellot 1965). Figure 6(*a*, *b*) shows the measured spectra in several experiments for different distances from the grid, expressed in the non-dimensional form $E(k_1)\epsilon^{-2/3}k_1^{5/3}$ versus $k_1\eta$, where η is the Kolmogorov lengthscale $(\nu^3/\epsilon)^{1/4}$; both E_w and E_u are presented. Note the presence of a well-defined inertial subrange for the w-component with α_2 agreeing with the previous results. Also note that the scaling employed collapses the dissipation subrange data well. However, the corresponding u-component did not fare as well as the w-component and showed deviations from $\alpha_1 = 0.51$, perhaps due to the contamination of the signal by longitudinal probe vibrations. The effects of noise are

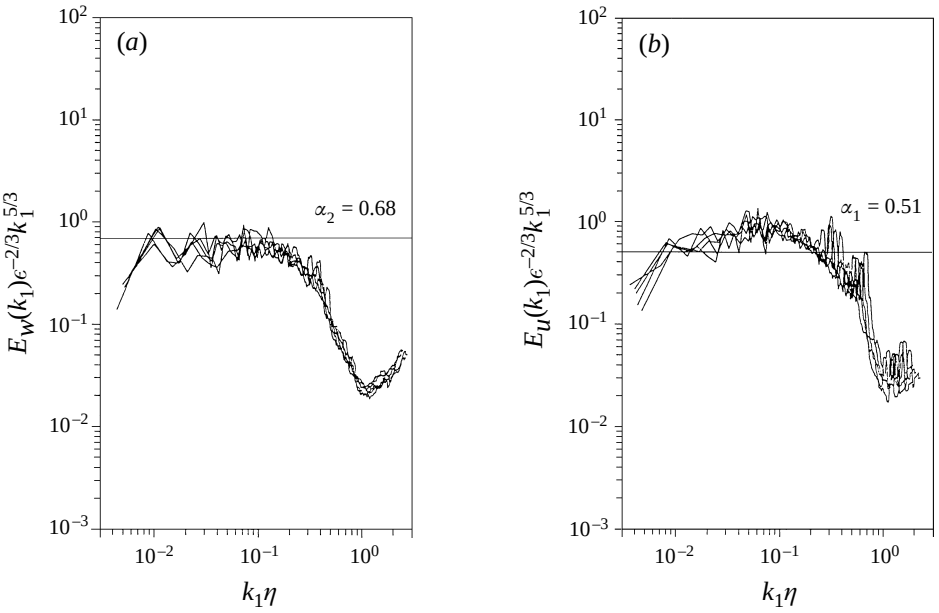

FIGURE 7. Same as figure 6, but for $f = 4.5$ Hz.

very clear in the high-wavenumber regime, where well-defined spikes are present. The anomalous skewness factor observed for u measurements, $S_K = 0.31$, reflects the presence of high-frequency noise. This trend was observed in all of the experiments, and is further illustrated using an additional set of measurements shown in figure 7(a, b). Inspection of the spectra presented by Brumley & Jirka (1987) indicate that both u- and w-components of their measurements have been contaminated by noise; see their figure 4. Because of the noise associated with our u-component measurements, it was decided to concentrate on the vertical velocity component measurements to interpret the data. The high-frequency noise seriously affects the measurement of fine-scale quantities but is expected to have a lesser effect on bulk quantities, such as r.m.s. velocities.

4. Measurements near density interfaces

4.1. *R.m.s. velocities*

The squares of r.m.s. velocity measurements (or the variance), $\overline{u^2}$ and $\overline{w^2}$, in the presence of a density interface are shown in figure 8(a), as a non-dimensional plot of $\overline{u^2}/u_H^2$ or $\overline{w^2}/w_H^2$ versus ξ/L_H. Here u_H^2 and w_H^2 correspond to the measurements in homogeneous fluids at the same location and ξ is the distance between the probe and the mean interfacial position. Previous LDV measurements of Hannoun *et al.* (1988) for $Ri = 70$ and 100 are also included for comparison. An amplification of the horizontal component and a monotonic reduction of the vertical component can be seen as the interface is approached. This modification is due to the strong suppression of vertical motions at the interface, which imposes additional kinematic and dynamical conditions on the motion field. The vertical motions at the interface are now constrained by buoyancy forces whose magnitude is on the order of Δb, which counter the inertial forces on the order of u_H^2/L_H associated with turbulent

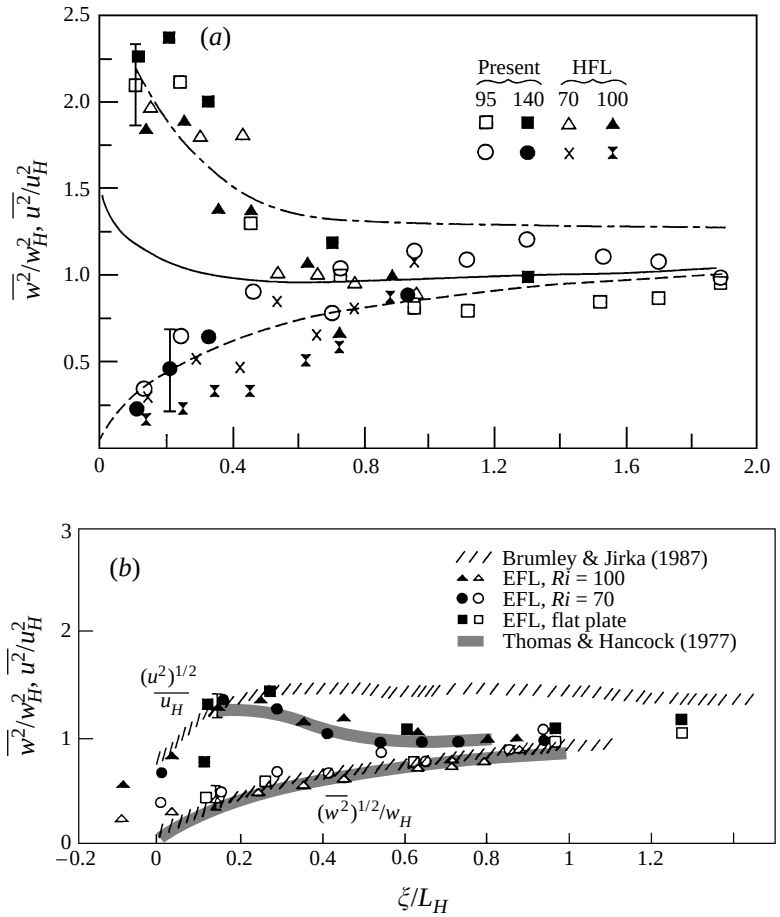

FIGURE 8. (*a*) The normalized variance of the vertical and horizontal velocity components versus the normalized distance from the density interface. The r.m.s. velocities and integral lengthscale in homogeneous fluids have been used for renormalization. The dashed and solid lines correspond to the theoretical relations obtained by Hunt & Graham (1978) for vertical and horizontal components, respectively. The dashed chain line corresponds to the nonlinear correction to the Hunt & Graham (1978) solution by Hunt (1984). HFL is the abbreviation for the data from Hannoun *et al.* (1988) taken at various *Ri*. (*b*) A summary of some previous turbulence data obtained near density interfaces and solid boundaries. The data include those of Thomas & Hancock (1977), Brumley & Jirka (1987), and Hannoun *et al.* (1988). The solid symbols represent the *u*-component of velocity.

motions. The ratio between these opposing factors is the Richardson number $Ri = \Delta b/(u_H^2/L_H) = \Delta b L_H/u_H^2$, which determines the nature of the density interface.

According to Perera, Fernando & Boyer (1994), a density interface subjected to an adjacent turbulent layer may look different depending on *Ri*, as follows.

(i) When Ri < 5 (approximately), the turbulence does not feel the stratification; here the turbulent front propagates into the non-turbulent layer as if no stratification were present.

(ii) When $5 <$ Ri < 30, the stratification is felt by the eddies of integral scales. These eddies impinge on the interface, penetrate a distance proportional to $L_H Ri^{-1}$ and splash the non-turbulent buoyant fluid into the turbulent layer. The fluid entrained in such a manner is broken down and mixed with the turbulent layer fluid.

(iii) When Ri > 30, the eddies of integral scales cannot directly participate in the

entrainment processes, and the turbulent entrainment is greatly reduced. Interfacial mixing now occurs by intermittent breaking of interfacial waves that are excited at the interface by the mixed-layer eddies. The resonant modes of these waves grow and burst into small turbulent patches, which merge with the turbulent layer.

It is this latter case (Ri $>$ 30) we have considered in the present study (figure 1*b*). Because of the low entrainment rate under these conditions, turbulence measurements using hot-film probes are possible and the flow can be considered as quasi-stationary.

From the data shown in figure 8(*a*), it appears that at the Richardson numbers considered (95 and 140) the normalized r.m.s. velocities do not show a significant and systematic dependence on *Ri*, within the experimental errors. For $\xi/L_H < 1$, the *u*-component shows a slightly higher amplification at high *Ri*, but the *w*-component does not show such a trend. The trends of the data of Hannoun *et al.* (1988) are also similar to ours, although some differences can be seen in specific measurements. These differences can be attributed to a variety of factors such as possible horizontal inhomogeneity of oscillating grid turbulence (McDougall 1979) and weak secondary flows that can be present. Further, it should be noted that Hannoun *et al.* (1988) did not measure L_H, but calculated it using the measured Eulerian integral time scale τ_ϵ as $u_H\tau_\epsilon$. Although it is plausible that $u_H\tau_\epsilon \propto L_H$, there is no reason to expect a proportionality constant of unity. Thus, care must be taken in comparing the absolute values of data taken from different experiments.

Figure 8(*b*) shows a summary of the results of several previous investigations. These include the data of Hannoun *et al.* (1988) taken near density interfaces and solid boundaries (which provide a means of comparison between finite- and infinite-*Ri* cases), the data of Thomas & Hancock (1977) taken in a wind tunnel above a platform moving with the speed of the flow and those of Brumley & Jirka (1984) taken near and away from an air–water free surface in the presence of oscillating-grid turbulence in the water side. An experiment similar to Thomas & Hancock's (1977) has been previously reported by Uzkan & Reynolds (1967), but it is believed that the Reynolds numbers of these experiments were too low to show the amplification of the *u*-component, and hence are not included here. An amplification of the *u*-component and a sharp reduction of the *w*-component are evident in all of the experiments shown in figure 8(*b*). Further, from the data of Hannoun *et al.* (1988), it is evident that for $\xi/L_H > 0.1$ there is no appreciable difference between the modification of turbulence by a solid surface or a sharp density interface, although the motion fields very near the interface are markedly different for the two cases because of the presence of interfacial waves in the former case.

According to McGrath, Fernando & Hunt (1997) and Hannoun *et al.* (1988), these interfacial waves have a r.m.s. amplitude of $\overline{\zeta^2_i}^{1/2} \simeq 3.2L_H Ri^{-5/6}$ and a vertical r.m.s. velocity of $\overline{w^2_i}^{1/2} \simeq 1.8u_H Ri^{-1/3}$. For typical Richardson numbers used in the present study, $Ri \simeq O(100)$, it is possible to expect $\overline{\zeta^2_i}^{1/2} \simeq 0.07L_H$ and $\overline{w^2_i}^{1/2} \simeq 0.4u_H$. The back-effects of these fluctuations on the turbulent layer (at large distances) are expected to be small compared to the overall damping effect introduced by the interface. According to Fernando & Hunt (1997), the spectra of wave-induced velocity fluctuations in the turbulent layer decay as $\Theta(k_1, z) \simeq \mathrm{e}^{-c_1(z/L_H)Ri}$, where c_1 is a constant of order one. This may be why the turbulent layers above high-*Ri* density interfaces and solid walls tend to have similar properties. Of course, close to the interface, $(\xi/L_H) < 0.1$, the nature of the turbulence is different for the two cases with, as $\xi \to 0$, the rigid surface having $u = w = 0$ and the density interface having the properties of interfacial waves.

The mechanisms leading to the modification of turbulence near density interfaces are of interest. Explanations based on RDT assume that the interface has a kinematic effect on the flow. For example, Hunt & Graham (1978) considered the effects of the sudden insertion of a rigid flat surface into homogeneous turbulence. In the inviscid limit, this is equivalent to the sudden generation of irrotational fluctuations in the flow, thus forcing the normal velocity component at the wall to zero. For short times following the insertion ($< L_H/u_H$), the vortex structures are not affected by these irrotational fluctuations and the flow can be considered as a superposition of the original homogeneous turbulence and the irrotational flow field. The induced irrotational field has more activity at small wavenumbers so that the cumulative effect is a significant modification of spectra at corresponding wavenumbers. Concurrently, the integral scales of turbulence for various velocity components change substantially, although there is no exchange of energy between wavenumbers. At large times nonlinear vortex stretching becomes important and solutions based on the superposition of homogeneous turbulence and irrotational distortions become invalid, and energy transfer between various wavenumbers should be considered. Although the Hunt & Graham (1978) approach is valid only for the initial adjustments of the flow, Hunt (1984) has shown that the resulting solutions are valid even at large times, if the dissipation is spatially uniform in shear-free boundary layers. As stated in § 1, the measurements taken near the atmospheric inversion layers show that indeed this may be the case (Caughey & Palmer 1979).

In figure 8(*a*), the Hunt & Graham solutions for $\overline{u^2}$ and $\overline{w^2}$ are shown by solid and dashed lines, respectively. Note that although the w-component agrees reasonably well with the theoretical prediction, the prediction for the u-component underestimates the results by a factor of 2 near the interface. The higher values of $\overline{u^2}/u_H^2$ observed near the interface can be attributed to the nonlinear (stretching of eddies) and viscous effects near the interface which are not included in the Hunt & Graham (1978) analysis. Hunt (1984) estimated the amplification that can be anticipated if the components of vorticity of eddies are systematically stretched and compressed by larger eddies of the size of integral scales. This correction does not have a significant effect on the w-component, but the u-component was shown to increase as

$$u^2 = u_H^2\left[1 + \frac{1}{3}\left(\frac{L_H}{z}\right)^{1/3}\right]. \tag{4.1}$$

The chain line shown in figure 8(*a*) corresponds to (4.1), which is in satisfactory agreement with the u-data for $\xi/L_H < 0.5$; beyond this distance, (4.1) overestimates the results. This is not unexpected because (4.1) is derived by assuming that the u-component has preferential amplification and the w-component is restrained by the 'wall blocking' effects. As ξ is increased, the wall blocking becomes less important and the flow appears to be dominated by pure kinematic effects induced by wall conditions.

A description alternative to the above notion of turbulence modification near density interfaces has been proposed by Long (1978), wherein turbulent eddies or blobs of fluid are assumed to flatten on the interface upon their impingement. In the recent work of Perot & Moin (1995), such impingement events have been called 'splats' and fluid parcels moving away from the boundary following the impingement events were termed 'antisplats'. As blobs of different scales impinge on the interface, they distort and transfer energy from the vertical components to the horizontal ones

via pressure scrambling effects. Thus, at a distance ξ, eddies of size greater than ξ are expected to be distorted by the interface, and those of size less than ξ should be free of distortions. Here also the vortex dynamics is important and the physical picture is different from that of Hunt & Graham (1978).

At this juncture, a brief discussion of the paper by Perot & Moin (1995) is warranted. They used direct numerical simulations (DNS) to study the nature of shear-free turbulence at different types of boundaries. The simulations were performed by inserting the solid surface into an isotropic, decaying, turbulent region. Although the existence of splats and antisplats were supported by their simulations, it was argued that it is neither the splats nor antisplats that cause intercomponent energy transfer, but the imbalance between the velocity fields associated with them. A splat transfers energy from the vertical to the horizontal component and, if there are no viscous effects, the horizontal motion continues until it meets the motion of another splat. The combined flow is deflected away from a wall, initiating an antisplat. Thus, in an average sense, there will be only little net energy transfer from the vertical to horizontal motions. They further argued that, when the viscous dissipation near the boundary is present, the tangential energy input to antisplats is only a fraction of that associated with splats, and this imbalance appears as a net energy transfer from the vertical to the horizontal components. Based on this argument, no amplification of $\overline{u^2}/u_H^2$ was expected as there will be no net energy input from w- to u-components.

However, an amplification of $\overline{u^2}/u_H^2$ was observed in the study of Perot & Moin (1995); they concluded that this is not a real flow phenomenon, but rather an artifact of the inhomogeneity of the dissipation. Their simulations show that the rate of dissipation ϵ is substantially less near the boundary, and hence the decay rate of $\overline{u^2}$ at the boundaries is much less than that of the deep interior of the flow (u_H^2). Thus, $\overline{u^2}/u_H^2$ tends to show an amplification, which is unrelated to the intercomponent energy transfer due to flattening of eddies. The Reynolds numbers of the simulations of Perot & Moin (1995) were relatively small to study inertial effects of eddies, although there was a single experiment carried out with a higher Reynolds number which showed no amplification, thus corroborating the above claim. However, in this run, the data were averaged only over two realizations, and the statistics so obtained are questionable. These authors further conjectured that the amplification of the streamwise velocity component observed in the experiments of Thomas & Hancock (1977) was not due to the intercomponent energy transfer, but due to the small amount of residual mean shear present in the experiments.

The above argument of Perot & Moin (1995) is not applicable to the present case because both $\overline{u^2}$ and u_H^2 have been measured under steady conditions. Yet, the data clearly show an amplification of $\overline{u^2}$ and a marked decrease of $\overline{w^2}$ near the interface. Thus we may conclude that the intercomponent energy transfer of eddies near high-Ri interfaces or solid walls is real. In addition, underestimation of our data by the theory of Hunt & Graham (1978) and the satisfactory agreement of data with Hunt's (1984) nonlinear correction indicate that nonlinear vortex stretching processes and 'flattening' of eddies near the interface play an important role in determining the u-component.

4.2. *Integral lengthscale*

The behaviour of integral lengthscales near the interface is of interest, as they determine the scales of wave motion at the interface as well as energy flux divergence. In the case of a solid boundary with $Ri \to \infty$, $w \to 0$ at the wall, and at a distance

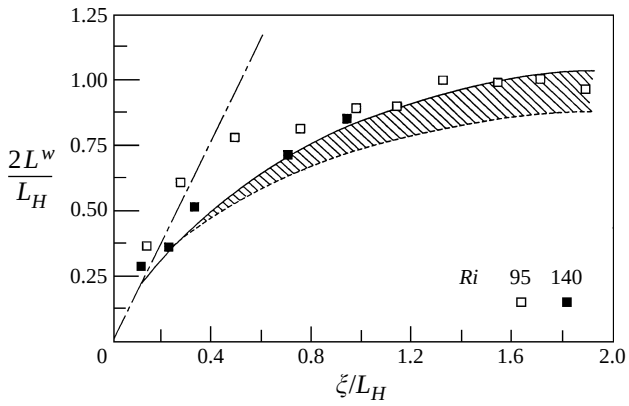

FIGURE 9. The longitudinal integral lengthscale of the vertical velocity component (normalized by its homogeneous counterpart) as a function of the distance from the density interface (normalized by the integral lengthscale for the homogeneous case). The dashed line corresponds to the relationship proposed by Hunt & Graham (1978). The shaded region corresponds to the atmospheric data taken from Hunt (1984). The dashed chain line corresponds to the atmospheric measurements of Caughey & Palmer (1979) which indicate $L^w \propto \xi$ near the interface (also see (4.4)).

$\xi(< L_H)$ the eddies that are not blocked by the interface are expected to contribute to the w-component. These latter eddies will have a wavenumber $k > \xi^{-1}$, and wavenumbers below ξ^{-1} are expected to be blocked. Thus, it is possible to expect (Hunt 1984)

$$L^w \to 0 \quad \text{as} \quad \xi \to 0, \tag{4.2}$$

and

$$E_w(k_1 \to 0) = \frac{\overline{w^2} L^w}{\pi} = \gamma_1 \epsilon^{2/3} \xi^{5/3} \quad (\xi < L_H) \tag{4.3}$$

where γ_1 is a constant. Furthermore, at a distance ξ, $\overline{w^2} \propto \epsilon^{2/3}\xi^{2/3}$, and hence using (4.3)

$$L^w = \gamma_2 \xi, \tag{4.4}$$

where γ_2 is a constant; Hunt (1984) estimated $\gamma_1 \simeq 1.125$ and $\gamma_2 \simeq 1.96$. Estimates have also been made for the horizontal components near the interface, which show that the spectrum $E_u(k_1 \to 0) = \overline{u^2} L^u/\pi$ is not drastically affected by the presence of the interface. The modified horizontal lengthscale becomes

$$L^u = L^u_H \left(\frac{u_H^2}{\overline{u^2}(\xi)} \right), \tag{4.5}$$

which indicates that the effect of a boundary is remarkably less pronounced for L^u compared to that of the vertical component. When $\xi \to 0$, $\overline{u^2}(0) \simeq 3/2 u_H^2$ and L^u is expected to decrease by a factor of $2/3$ from its homogeneous counterpart. Similar (qualitative) trends can be anticipated if one assumes the existence of splats and antisplats. Here, the strongly divergent flow near the interface is expected to decrease the u-component, and hence L^u.

Figure 9 shows the measurements of L^w, presented in non-dimensional form. The atmospheric measurements presented in Hunt (1984) are also shown in the figure, which show a fair agreement with our data. For small ξ ($< 0.5\ L_H$), the form (4.4) based on 'blocking effects' of eddies is well substantiated and apparently there is no

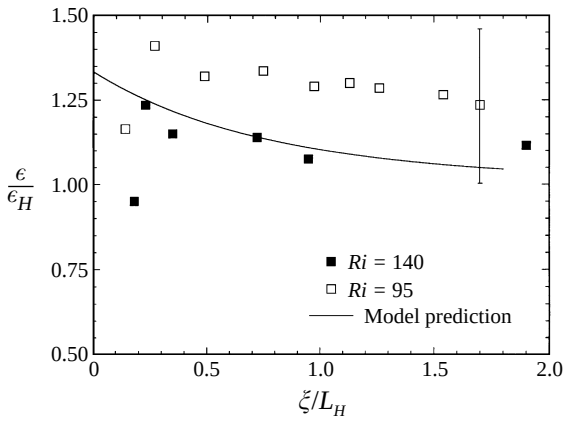

FIGURE 10. The rate of dissipation of turbulent kinetic energy (normalized by its value for the homogeneous case) as a function of distance from the density interface (normalized by the integral lengthscale for the homogeneous case). The solid line indicates the prediction of (4.7) based on a simple model.

measurable influence of interfacial waves on L^w. The predictions of Hunt & Graham (1978) coresponding to $Ri \to \infty$ consistently underestimate the data for $\xi > 0.2L_H$. The pronounced influence of nonlinear vortex stretching and the enhanced vertical energy transports by viscous effects near the interface (as noted by Perot & Moin 1995) may have caused dramatic changes to the flow near the interface, thus making it far from the conditions required for the RDT analysis to be valid. Measurement of L^u similarly showed a decrease near the interface, but because of possible noise contamination these results are not presented here.

4.3. *Dissipation*

As stated in §2, the rate of dissipation measurements were made at different distances from the interface, as the interface migrated away from the probe. Note that during these measurements the probe location with respect to the grid was constant and, hence, the rate of dissipation ϵ_H corresponding to the homogeneous case was held constant. The effect of the interface on the dissipation can be evaluated by comparing ϵ and ϵ_H, at different distances ξ from the interface. Figure 10 shows a plot of ϵ/ϵ_H versus ξ/L_H for two different Richardson numbers ($Ri = \Delta b L_H/u_H^2$). Several interesting aspects can be noted in these measurements.

First, ϵ near the interface appears to decrease rapidly, sometimes falling below its corresponding homogeneous counterpart. This region is expected to be affected by the viscous effects, because of the flattening of eddies above the interfaces causing the development of a viscous boundary layer. Horizontal sloshing motions of the eddies feel the boundary effects of the interface through this layer. Estimates of Hunt (1984) indicate that the thickness of this viscous boundary layer δ_v can be given by $\delta_v \sim L_H Re^{-1/2}$; from our experiments the proportionality constant can be evaluated as 2.5, based on the typical values of $Re \simeq 100$, $\delta_v/L_H \simeq 0.25$. Simulations of Perot & Moin (1995) also indicate a drop of ϵ near an ideal free surface, which was attributed to the tendency of turbulence to achieve two-component characterization (i.e. $w = 0$) near an interface.

Second, ϵ/ϵ_H is consistently high in the bulk of the turbulent layer, even away from the source layer (i.e. at $\xi \geqslant L_H$). This indicates the possibility of turbulence

adjusting over the entire turbulent layer, although the bulk velocity and lengthscale adjustments are confined mainly to $\xi < L_H$ (it is, however, clear from figure 8(a, b) that the turbulent layer velocities can remain unequal to u_H even beyond $\xi = L_H$, although their variations are small). This observation can be attributed to the accumulation of turbulent kinetic energy produced by the grid in the mixed layer topped by the density interface. If there were no interface, this additional energy could have propagated past the interface into the deep interior as a consequence of the non-zero energy flux divergence term in the kinetic energy equation.

It is unlikely that the amount of turbulent kinetic energy produced by the grid is altered by the presence of the interface, if all other grid conditions remain the same. If an interface is inserted into an unbounded homogeneous fluid layer in which the turbulence is driven by an oscillating grid, so that the new turbulent layer is confined to a depth D, then the extra dissipation $\Delta\epsilon$ that is retained in the turbulent layer should be equal to that corresponding to the region $D < z < \infty$ of the homogeneous fluid. Assuming that the dissipation in homogeneous fluids scales as $\epsilon = \gamma_3 K^3/z^4$, where γ_3 is a constant and K is the 'action' parameter (defined by Long 1978, as $K = \overline{u^2}^{1/2} z$, which is a constant since $\overline{u^2}^{1/2}$ goes as z^{-1} for grid turbulence), and that the extra dissipation is uniformly distributed, it is possible to write

$$\Delta\epsilon = \gamma_3 K^3/3D^4. \tag{4.6}$$

The new dissipation ϵ at a distance z from the grid thus becomes

$$\epsilon/\epsilon_H = \left[1 + \tfrac{1}{3}\left(z/D\right)^4\right]. \tag{4.7}$$

Note that the calculation leading to (4.7) is only approximate and neglects the modification of ϵ over the viscous layer δ_v. It is evident that for typical experimental conditions (where the homogeneous turbulence is measured in a deep fluid layer of depth much greater than D) $\epsilon > \epsilon_H$, and the ratio ϵ/ϵ_H should decrease as the interface propagates away from the probe during a given experiment. An estimate of ϵ/ϵ_H based on (4.7) is also indicated in figure 10 by a solid line. Although the data for $Ri = 140$ follow (4.7) for $\xi > \delta_v$, the data for $Ri = 95$ consistently lie above (4.7), but mostly within the $\pm 15\%$ error margin of ϵ and ϵ_H measurements. If the energy flux divergence for the flow were zero (homogeneous turbulence), then one would have expected that $\Delta\epsilon = 0$ and the dissipation in the bulk of the mixed layer for $\xi > \delta_v$ to be a constant. This conclusion is also borne out by the DNS data of Perot & Moin (1995). Thus, the bane for the RDT calculations is the presence of a thin, yet prominent, viscous sublayer near the interface and the involvement of nonlinear vortex dynamics which weakens the assumption of irrotational distortions at large times of evolution.

4.4. *Spectra*

Measurements of spectra at different distances from the interface were made using the rotating hot-film probe. A typical set of such spectra for the vertical $E_w(k_1)$ and horizontal $E_u(k_1)$ velocity fluctuations is shown in figure 11(a, b) for $Ri = 95$. When comparing figures 6(a, b) and 7(a, b) with figure 11(a, b), several distinct features with respect to the modification of turbulence near the interface are evident. Beyond $\xi/L_H = 0.5$, the inertial subrange appears to be relatively free from the interfacial distortion effects. At all ξ/L_H, Kolmogorov scales in the dissipation subrange are unaffected by the interface. Qualitative comparison of figures 11(a) and 11(b) shows that the interfacial effects are more pronounced in the $E_w(k_1)$ spectra. The distortion

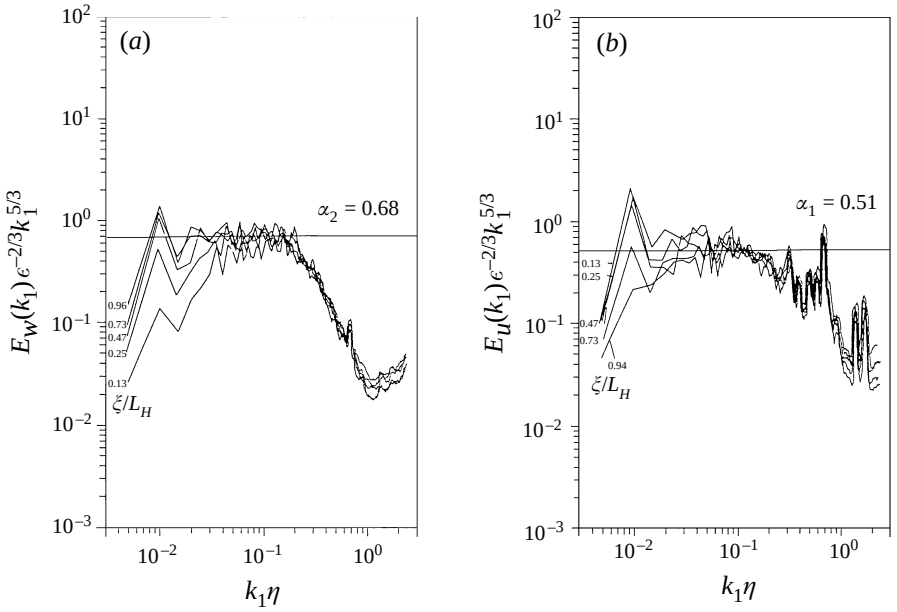

FIGURE 11. The normalized kinetic energy wavenumber spectra measured at various normalized distances ξ/L_H from the interface at $Ri = 95$. (*a*) Vertical velocity component, (*b*) horizontal velocity component.

of turbulence occurs mainly at the low-wavenumber end of the inertial subrange scales, wherein the kinetic energy of the vertical component decreases while that of the horizontal component increases. As the interface is approached, more and more scales of the inertial subrange are distorted and very near the interface (say $\xi/L_H \leqslant 0.2$) an inertial subrange hardly exists. The same trends were also observed in the experiments carried out at $Ri = 140$.

According to the RDT calculations of Hunt & Graham (1978) and Hunt (1984), the blocking effects are felt when $\xi < L_H$ at wavenumbers $k < L_H^{-1}$, whence the spectra tend to flatten according to (4.3). For $k > L_H^{-1}$, the spectra take the Kolmogorov form (3.1). The results presented in figure 11(*a*) are in qualitative agreement with these predictions, but there are quantitative disparities. For example, although the RDT calculations show that $E_u(k_1 \ll L_H^{-1})$ should be unaffected by the presence of the interface, the experimental results show that appreciable changes occur at $k_1 \to 0$ for $E_u(k_1)$. In particular, the kinetic energy of the lower wavenumbers is seen to be increased in the experiments. This observation, together with the data and their comparison with theoretical predictions, underscores the importance of accounting for the nonlinear and viscous effects near the interface.

As mentioned in §3.1, an alternative description for turbulence near interfaces is based on blobs (eddies) of fluid impinging on the interface that transfer energy from the vertical to horizontal motions. At a given ξ, eddies of size $k^{-1} > \xi$, are influenced by the interface. The observation that both *w*- and *u*-component spectra at small wavenumbers are modified by the interface is consistent with this picture. Hannoun *et al.* (1988) have also measured the Eulerian frequency spectra $E_w(\omega)$ and $E_u(\omega)$ in the proximity of density interfaces, in the region $0.14 < \xi/L_H < 1.5$, and reported evidence for intercomponent energy transfer from *w*- to *u*-components. However, they did not report the effect of an interface on inertial and dissipation subranges, nor

measured dissipation ϵ near the interface. The present work complements their work and provides more details on the nature of turbulence near interfaces.

5. Summary and discussion

The results of an experimental study carried out to investigate the properties of zero-mean-shear turbulence near density interfaces are described in this paper. An oscillating-grid mixing-box experiment was used for this purpose, and the measurements were made in the lower turbulent layer of a two-layer fluid using a rotating hot-film probe. Special attention was given to the study of how a shear-free turbulent flow is distorted by the introduction of an interface with the hope of applying results to the modelling of turbulence near density interfaces.

In particular, the results were compared with the rapid distortion theory (RDT) based calculations of Hunt & Graham (1978) and Hunt (1984) that deal with the distortion of turbulence near solid surfaces. Although there are marked discrepancies between the assumptions of the theory and the experimental conditions, some broad similarities exist between the experimental and theoretical flow configurations; hence, the RDT predictions were considered to be a useful tool in the interpretation of the experimental observations. To facilitate comparisons between the theory and experiments, the turbulence was first measured in an unstratified fluid layer, and then the measurements were repeated with a strong density interface while the grid forcing remains the same. The Richardson numbers used in the experiments ($Ri = \Delta b L_H / u_H^2$, where Δb is the buoyancy jump, L_H is the integral scale and u_H is the r.m.s. velocity) were 95 and 140, thus ensuring that the internal wave amplitude and the interfacial migration rates are small compared to integral length and velocity scales, respectively, of turbulence. The salient results of the present study can be summarized as follows.

(i) The introduction of a density interface into a mean shear-free turbulent flow distorts the structure of turbulence around it. The modifications of velocity and lengthscales of turbulence are felt to a distance of the order of one integral lengthscale wherein the horizontal velocity component is amplified and the vertical component is suppressed. The modification of the rate of change of kinetic energy, however, was felt over distances greater than L_H. The longitudinal lengthscale L^w of the vertical velocity component w was found to have a linear relationship with the distance from the interface, $L^w \sim \xi$ for $\xi < 0.5 L_H$. The r.m.s. vertical velocity for the stratified case was found to be well predicted by the RDT calculations of Hunt & Graham (1978) and Hunt (1984) which were mainly derived for solid boundaries. The magnitude of the u-component of velocity, however, was underpredicted although the trend of data was consistent with their calculations. The RDT calculations neglect the nonlinear vortex dynamics near the interface, which appears to be an important element in determining the u-component. The nonlinear model proposed by Hunt (1984) described the u-data near the interface more satisfactorily.

Since the w-velocity component plays a major role in determining the dynamics of the interface (Carruthers & Hunt 1986), RDT estimates are expected to be reasonable for the interfacial properties such as vertical velocities and amplitudes of internal waves. The lengthscale L^w was also underpredicted by the RDT calculations, although the qualitative trends of the predictions and measurements were similar. This can be attributed to the additional complexities that arise in the experiments due to nonlinear vortex stretching and viscous effects near the interface.

Comparison of present data with those taken near solid surfaces by Hannoun *et al.*

(1988) shows that the effects of interfacial wave motions are felt up to a distance $\xi \sim 0.1L_H$.

(ii) The effects of the interface are felt mainly at large scales of turbulence. Depending on the distance ξ to the interface, eddies of either integral scale or from the low-wavenumber end of the inertial subrange are distorted so that the kinetic energy of the vertical velocity component is reduced and that of the corresponding wavenumber regions of the horizontal component is enhanced. Very near the interface ($\xi < 0.15L_H$), the entire inertial subrange is distorted; practically all turbulent scales of the original undistorted inertial subrange show deviation from the $k^{-5/3}$ spectrum. The Kolmogorov scale eddies of the dissipation subrange appear to remain undistorted at all distances from the interface.

The measured longitudinal spectrum of the vertical velocity E^w shows at least qualitative similarities to those predicted by the RDT calculations, in that the large wavenumbers show $k^{-5/3}$ behaviour and smaller ones are drastically distorted. However, the spectra for horizontal velocity E^u showed different behaviour. Contrary to the RDT prediction of no change at $E^u(k_1 \to 0)$, the measurements showed an increase of $E^u(k_1)$ at low wavenumbers. This observation provides further support for the notion that the nonlinear vortex stretching is important near the surface wherein the horizontal velocity components are expected to amplify at integral scales. The results are also consistent with the concept of eddies (or splats) impinging and flattening at the interface, thus transferring the energy of the vertical component to the horizontal components. Based on simulations of decaying turbulence near interfaces, Perot & Moin (1995) proposed that such splats (and antisplats) exist, but the viscous effects near the boundary can inhibit the amplification of the horizontal component. Our results indicate that the amplification of the u-component is indeed tenable.

(iii) The rate of turbulent kinetic energy dissipation ϵ near the interface shows a sharp decrease. The collapse of data at dissipation scales, taken at different ξ, indicates that the dissipating scales follow Kolmogorov scaling although the large-scale turbulence near the interface is anisotropic. Away from the interface ($\xi > 0.25L_H$), ϵ increases to values greater than the corresponding homogeneous case. This increase could be attributed to the confinement of turbulent kinetic energy produced by the grid to a smaller volume determined by the density interface. As stated in (i), the effects of increased dissipation are felt well beyond $\xi = L_H$, and a simple calculation suggests that this increase may be uniformly distributed over the entire turbulent layer. Further, the calculations point to the possibility that, if an interface is introduced into homogeneous turbulence, then the dissipation approximately remains unchanged except within a thin viscous layer ($\delta_v \sim 2.5L_H Re^{-1/2}$) near the interface.

The available RDT analyses are based on the inviscid calculations and disregard the existence of this viscous layer. Then, an assumption is made that the dissipation above the interface remains constant with height, and hence the distortion of homogeneous turbulence by the introduction of the interface is equivalent to the addition of an irrotational velocity field. However, the present work suggests that the viscous effects and nonlinear vortex stretching near the interface may play an important role in determining at least the horizontal velocity field near the interface.

We would like to thank the referees for insightful comments that led to significant improvements of the paper. Stratified turbulent flow research at Arizona State University is sponsored by the the Office of Naval Research (Small-Scale Mixing and High Latitude Programs), US National Science Foundation, Army Research Office (DAAH-04-95-1-0132) and the Environmental Protection Agency (Office of

Exploratory Research). The authors wish to gratefully acknowledge this support. Technical support was provided by Dr C. Y. Ching and Mr Leonard Montenegro.

REFERENCES

Brumley, B. H. & Jirka, G. H. 1987 Near surface turbulence in a grid-stirred tank. *J. Fluid Mech.* **183**, 235–263.

Carruthers, D. J. & Hunt, J. C. R. 1986 Velocity fluctuations near an interface between a turbulent region and a stably stratified layer. *J. Fluid Mech.* **165**, 475–501.

Carruthers, D. J. & Hunt, J. C. R. 1997 Waves, turbulence and entrainment near an inversion layer. Submitted.

Caughey, S. J. & Palmer, S. G. 1979 Some aspects of turbulence through the depth of the convective boundary layer. *Q. J. R. Met. Soc.* **110**, 13–34.

Comte-Bellot, G. 1965 Ecoulement turbulent entre deux parois paralleles. *Publications Scientifiques et Techniques du Minister de l'Air*. No 419. Paris.

Fernando, H. J. S. & Hunt, J. C. R. 1997 Turbulence, waves and mixing at shear-free interfaces. Part 1. A theoretical model. *J. Fluid Mech.* Submitted.

Gargett, A. E., Osborn, T. R. & Nasmyth, P. W. 1984 Local isotropy and the decay of turbulence in a stratified fluid. *J. Fluid Mech.* **144**, 231–280.

Hannoun, I. A., Fernando, H. J. S. & List, E. J. 1988 Turbulence structure near a sharp interface. *J. Fluid Mech.* **189**, 189–209.

Hinze, J. O. 1975 *Turbulence*. McGraw-Hill.

Hopfinger, E. J. & Linden, P. F. 1982 Formation of a thermocline in zero-mean-shear turbulence subjected to a stabilizing buoyancy flux. *J. Fluid Mech.* **114**, 157–173.

Hopfinger, E. J. & Toly, J. A. 1976 Spatially decaying turbulence and its relation to mixing across density interfaces. *J. Fluid Mech.* **78**, 155–175.

Hunt, J. C. R. 1984 Turbulence structure in thermal convection and shear-free boundary layers. *J. Fluid Mech.* **138**, 161–184.

Hunt, J. C. R. & Graham, J. M. R. 1978 Free-stream turbulence near plane boundaries. *J. Fluid Mech.* **84**, 209–235.

Kit, E., Fernando, H. J. S. & Brown, J. A. 1995 Experimental examination of Eulerian frequency spectra in zero-mean-shear turbulence. *Phys. Fluids* A **7**, 1170–1188.

McDougall, T. J. 1979 Measurements of turbulence in a zero-mean-shear mixed layer. *J. Fluid Mech.* **94**, 409–430.

McGrath, J. L., Fernando, H. J. S. & Hunt, J. C. R. 1996 Turbulence, waves and mixing at shear-free interfaces. Part 2. Laboratory experiments. *J. Fluid Mech.* Submitted.

Long, R. R. 1978 A theory of mixing in stably stratified fluids. *J. Fluid Mech.* **84**, 113–124.

Perera, M. J. A. M., Fernando, H. J. S. & Boyer, D. L. 1994 Turbulent mixing at an inversion layer. *J. Fluid Mech.* **267**, 275–298.

Perot, B. & Moin, P. 1995 Shear-free turbulent boundary layers. Part 1. Physical insights into near-wall turbulence. *J. Fluid Mech.* **295**, 199–227.

Sreenavasan, K. 1984 On the scaling of the turbulence energy dissipation rate. *Phys. Fluids* **27**, 1048–1051.

Tavoularis, S., Bennett, J. C. & Corrsin, S. 1978 Velocity-derivative skewness in small Reynolds number, nearly isotropic turbulence. *J. Fluid Mech.* **88**, 63–69.

Tennekes, H. & Lumley, J. L. 1972 *A First Course in Turbulence*. The MIT Press.

Thomas, N. H. & Hancock, P. E. 1977 Grid turbulence near a moving wall. *J. Fluid Mech.* **82**, 481–496.

Thompson, S. M. & Turner, J. S. 1975 Mixing at an interface due to turbulence generated by an oscillating grid. *J. Fluid Mech.* **67**, 348–368.

Turner, J. S. 1968 The influence of molecular diffusivity on turbulent entrainment across a density interface. *J. Fluid Mech.* **33**, 639–656.

Uzkan, T. & Reynolds, W. C. 1967 A shear-free turbulent boundary layer. *J. Fluid Mech.* **28**, 803–821.